Virus-Mediated Knockdown of Nav1.3 in Dorsal Root Ganglia of STZ-Induced Diabetic Rats Alleviates Tactile Allodynia

Andrew M Tan,[*] Omar A Samad,[*] Sulayman D Dib-Hajj, and Stephen G Waxman

Department of Neurology, Yale University School of Medicine, New Haven, Connecticut, United States of America; and Center for Neuroscience and Regeneration Research, Veterans Affairs Connecticut Healthcare System, West Haven, Connecticut, United States of America

Diabetic neuropathic pain affects a substantial number of people and represents a major public health problem. Available clinical treatments for diabetic neuropathic pain remain only partially effective and many of these treatments carry the burden of side effects or the risk of dependence. The misexpression of sodium channels within nociceptive neurons contributes to abnormal electrical activity associated with neuropathic pain. Voltage-gated sodium channel Nav1.3 produces tetrodotoxin-sensitive sodium currents with rapid repriming kinetics and has been shown to contribute to neuronal hyperexcitability and ectopic firing in injured neurons. Suppression of Nav1.3 activity can attenuate neuropathic pain induced by peripheral nerve injury. Previous studies have shown that expression of Nav1.3 is upregulated in dorsal root ganglion (DRG) neurons of diabetic rats that exhibit neuropathic pain. Here, we hypothesized that viral-mediated knockdown of Nav1.3 in painful diabetic neuropathy would reduce neuropathic pain. We used a validated recombinant adeno-associated virus (AAV)-shRNA-Nav1.3 vector to knockdown expression of Nav1.3, via a clinically applicable intrathecal injection method. Three weeks following vector administration, we observed a significant rate of transduction in DRGs of diabetic rats that concomitantly reduced neuronal excitability of dorsal horn neurons and reduced behavioral evidence of tactile allodynia. Taken together, these findings offer a novel gene therapy approach for addressing chronic diabetic neuropathic pain.
Online address: http://www.molmed.org
doi: 10.2119/molmed.2015.00063

INTRODUCTION

Diabetic neuropathic pain is a chronic and often intractable condition with limited clinical treatment options and represents a major unmet medical need (1). A large body of work demonstrates that abnormal sodium channel expression in dorsal root ganglion (DRG) neurons produces hyperexcitability in these neurons that underlies neuropathic pain (2,3). Emerging evidence has demonstrated that the voltage-gated sodium channel isoform Nav1.3 has an important role in the development and maintenance of neuropathic pain (4–6). Nav1.3 is a tetrodotoxin-sensitive (TTX-S) sodium channel and produces sodium currents with rapid repriming kinetics that can contribute to neuronal hyperexcitability and enhance repetitive firing characteristics and ectopic firing in injured neurons (7,8). Although Nav1.3 is normally undetectable in adult DRG neurons, expression of this sodium channel subtype is upregulated in these cells after axotomy (that is, nerve transection) and chronic constriction injury models of neuropathic pain (4,6,7,9–11). Previous studies have

shown that levels of Nav1.3 increase in DRG neurons of streptozotocin (STZ)-induced diabetic models of neuropathic pain (12). Thus, it has been posited that Nav1.3 upregulation within DRG neurons in diabetes contributes to hyperactivity of nociceptive circuits and neuropathic pain (13). Here, we hypothesize that knockdown of Nav1.3 will reduce neuropathic pain in painful diabetic neuropathy. Specific targeting of sodium channel isoforms as a strategy for treating neuropathic pain has been particularly difficult owing to the absence of validated isoform-selective small-molecule inhibitors. The advent of gene therapy has recently shown promise in the treatment of neuropathic pain, particularly the use of viral-mediated delivery of small-hairpin RNA (shRNA) constructs to knockdown target proteins (5,14). In general, gene therapy offers three major advantages: target specificity (for example, blocking of specific sodium channel isoforms), reduced incidence of adverse events or side effects, and thera-
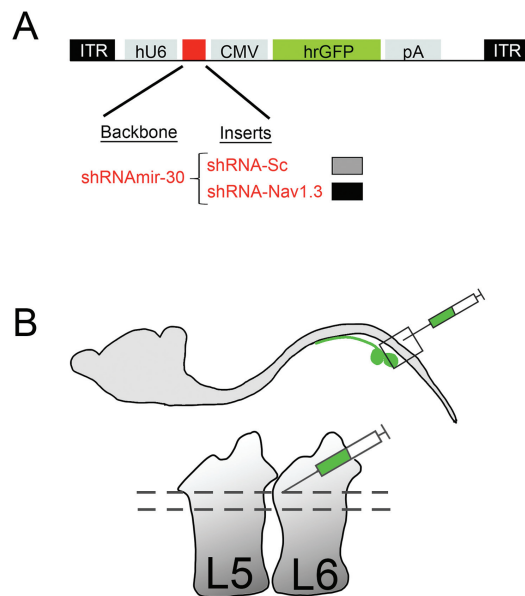
Figure 1. Intrathecal injection delivery of AAV vectors. (A) A diagram showing the AAV-shRNA vector used to target Nav1.3 *in vivo* (adapted from Samad *et al.*, 2013 (5)). (B) A small laminectomy was performed between vertebral columns L5 and L6. AAV-vectors were then injected into intrathecal space and resulted in vector transduction of DRGs along the lumbar enlargement.

peutic durability (15). We have previously demonstrated that direct injection into DRG of adeno-associated virus (AAV) vectors expressing shRNA against Nav1.3 resulted in significant knockdown of Nav1.3 expression and reduced nerve injury–induced neuropathic tactile allodynia (5). This direct-DRG injection study demonstrated the proof of principle that a gene therapy approach to pain can be used with high transduction efficiency. Intra-DRG delivery of the knockdown construct offers flexibility through its limited segmental disease-modifying effects on pain-associated behavior but is less clinically relevant because of the invasive method of delivery. In this study, we assessed the translational potential of Nav1.3 knockdown by viral-mediated delivery of AAV-shRNA-Nav1.3 in diabetic neuropathic pain. We administered the vector using a clinically relevant intrathecal injection approach, a minimally invasive technique and a more applicable delivery strategy compared with direct-DRG injection. Three weeks following intrathecal injection in diabetic rats, we observed robust viral infection of multiple DRGs along the lumbar enlargement without infection of spinal cord neurons, reduced tactile allodynia, and a concomitant decrease in nociceptive dorsal horn neuron hyperexcitability. Together, these findings demonstrate for the first time the functional relevance of Nav1.3 misexpression in diabetic neuropathic pain and provide groundwork for developing targeted gene therapy to manage chronic pain.

MATERIALS AND METHODS

Animals

All experiments were performed in accordance with the National Institutes of Health Guidelines for the Care and Use of Laboratory Animals. All animal protocols were approved by the VA Connecticut Healthcare System Institutional Animal Care and Use Committee. Adult male Sprague Dawley rats (225–300 g; Harlan) were used in this study. Animals were housed in groups of two per cage and were kept in a room at a constant temperature (22°C) and relative humidity (60%) with alternating 12-h light–dark cycles. All experimental procedures were performed during the light cycle. Food and water were provided to animals *ad libitum*.

STZ-Induced Diabetes

All animals were injected with STZ (50 mg/kg body weight, intraperitoneally [IP]; Sigma-Aldrich), as described previously (16). STZ is a pancreatic β-cell toxin that produces type I diabetes (17). Glucose levels were measured from blood samples drawn from the ventral tail vein immediately at the end of the experiment, that is, at an endpoint 3 wks after STZ injection (OneTouch Ultra glucose monitoring system; LifeScan). Diabetes mellitus was defined as hyperglycemia with blood glucose of 250 mg/dL or higher (12). All animals included in our analyses developed significant hyperglycemia according to these inclusion criteria. As expected with this STZ-induced diabetes model, diabetic animals tended to lose body weight over the 2-wk course of the experiment (18). To maintain body mass, diabetic animals were provided with supplemental liquid food on a routine basis and allowed to feed *ad libitum* (Ensure, 150 mg daily; Abbott Laboratories). Animals were randomly assigned to two groups: those animals injected intrathecally with control AAV-shRNA-scrambled (-Sc) or with AAV-shRNA-Nav1.3 (also see below). All animals underwent blood glucose and behavioral testing. A subpopulation of animals was used for terminal electrophysiological testing. Tissue was collected for histological processing and analysis at the end of all experiments.

siRNA Design, Cloning, and Viral Vector

The siRNA design, sequence, cloning, and viral vector used in this study have been described previously (5) (also see Figure 1A). TTX-S currents in DRG neurons (in normal or diabetic animals) are a composite of Nav1.1, -1.3, -1.6 and -1.7, and physiological methods lack the resolution to distinguish the effect on any

single isoform within the composite current in primary neurons. Thus, to verify the specificity and efficacy of functional Nav1.3 knockdown with the construct, we measured sodium currents in cultured HEK293 cells that stably expressed rat Nav1.3 (5,13) and observed a several-fold reduction in the Nav1.3 current (5). The siRNA construct significantly decreased Nav1.3 mRNA levels as measured by reverse transcriptase polymerase chain reaction (RT-PCR) in DRG neurons and had no off-target effects on other members of the voltage-gated sodium channel family, including Nav1.6, -1.7, -1.8, or -1.9 (5).

The viral titers used in this study were as follows: AAV-shRNA-Sc, 7.27×10^{13} viral genomes (vg)/mL; AAV-shRNA-Nav1.3, 7.05×10^{13} vg/mL (Gene Transfer Vector Core, IA). Before the viral solutions were injected into diabetic animals, viral solutions were desalted using Slide-A-Lyser minidialysis according to manufacturer's instructions (Thermo Scientific). Desalting was done for 1 h at 4°C immediately prior to intrathecal injections in animals.

Intrathecal Injection

Animals were anesthetized via exposure to 1–3% isoflurane in oxygen. A small laminectomy (~1 mm^2) was performed between lumbar levels L5 and L6 to expose the thecal sac (16,17) (Figure 1B). This allowed visual confirmation that the needle entered the intrathecal space without damaging the spinal cord. To avoid injury to the underlying spinal cord tissue, the needle was kept at midline and slowly inserted at a very shallow angle (less than 30° to the surgical table) underneath the dura. Viral particles in a 5-uL volume were injected using a 10-μL Hamilton syringe with a 32-gauge needle. After injection, the paraspinal muscles and skin were sutured closed in layers using 4.0 silk sutures.

Immunodetection Methods

Immunohistochemical analyses on cryosections were performed as previously described (19) (Figure 2). Briefly, rats were deeply anesthetized with
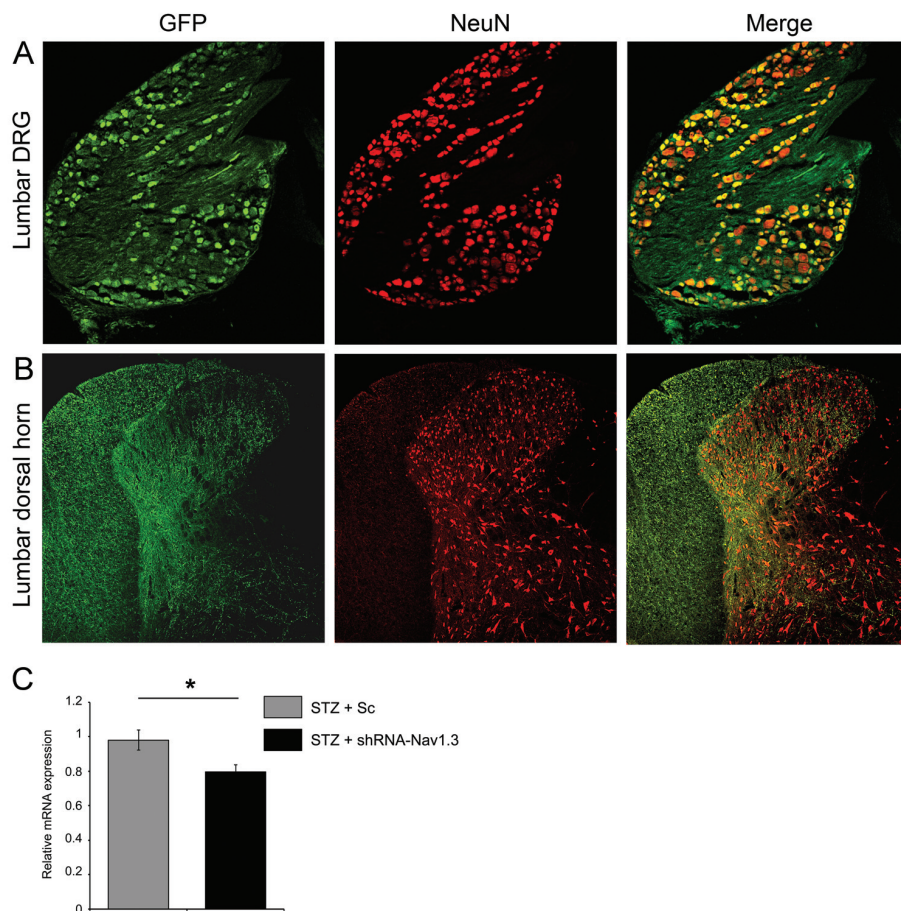

Figure 2. Intrathecal injection of AAV infects lumbar DRG neurons. Following intrathecal injections of AAV2/5 vectors (with GFP reporters). (A) DRG were stained with GFP and NeuN. A merged image in the top panel in A shows that cell bodies immunopositive for *GFP* (cells infected by vectors) colocalize with NeuN, as shown by yellow color. (B) A similar histological approach in spinal cord tissue from the same animals revealed no colocalization of GFP and NeuN, demonstrating that AAV vectors did not infect spinal cord neurons (see merged bottom panel in B). As expected, some GFP-labeled afferent fibers from infected DRGs appeared in the dorsal column white matter tracts and in the deeper laminae of the dorsal horn gray matter (white arrowheads). (C) Normalized Nav1.3 quantitative PCR from lumbar enlargement DRGs 3 wks after AAV intrathecal injection demonstrate significant differences in Nav1.3 mRNA expression following shRNA-Nav1.3 compared with scrambled AAV vector treatment.

ketamine/xylazine (75/5 mg/kg body weight; IP) and transcardially perfused with phosphate-buffered saline (PBS) followed by a 4% paraformaldehyde solution in 0.1 mol/L PBS. Rat spinal cord and DRGs from L4–L5 were collected. Sections were blocked with PBS containing 5% fish skin gelatin (Sigma-Aldrich), 6% normal donkey serum, 0.6% Triton X-100 and 0.02% sodium azide for 1 h at room temperature. Subsequently,

slides were incubated individually or in combination with primary antibodies. The following primary antibodies were used: rabbit anti–green fluorescent protein (GFP) (Invitrogen 1:1000) and mouse anti-NeuN (Millipore 1:1000). Sections were then incubated with secondary antibodies, donkey anti-mouse IgG-488 Dylight (Jackson ImmunoResearch) and donkey anti-rabbit IgG-Cy3 (Jackson ImmunoReasearch).

Pain Behavioral Assays

A blinded experimenter performed all behavioral experiments. All rats were acclimatized to the behavioral testing room in three to four habituation sessions. Baseline behavioral data were recorded 1–2 d prior to STZ injection (considered d 0). Subsequent behavioral testing was performed during wk 1 and at the experimental endpoint at wk 3. For tactile withdrawal threshold assessments, rats were placed on an elevated wire grid and the lateral plantar surface of the paw of each animal was presented with a series of calibrated Von Frey filaments (Stoelting). The withdrawal threshold (determined as 50% response rate) was determined using the "up-down" method for rats (16,20). For thermal sensitivity, the plantar surface of the paw was exposed to a radiant heat source using a Hargreaves apparatus (ITC) (21). Paw withdrawal latency was then measured (with initial beam intensity adjusted for a baseline withdrawal latency of 9–11 s). Thermal withdrawal latency testing was performed 3 times per animal (with a rest interval of at least 5 min). To prevent tissue damage, the radiant heat source in the apparatus was automatically cut off at 20.5 s. For all animals, tactile and heat threshold withdrawal data were averaged within groups and then compared across groups.

Electrophysiology

Animals were anesthetized with sodium pentobarbital (40 mg/kg, IP), and a laminectomy was performed to expose the spinal lumbar enlargement. The overlying dura was carefully excised and warm mineral oil was applied over the recording area. Core body temperature was monitored with a rectal thermometer and maintained (34°C ± 2°C) using a circulating water heating pad. Recordings were obtained with a low-impedance 5-mΩ tungsten-insulated microelectrode (A-M Systems) that was positioned near the L4/L5 dorsal root entry zone. Electrical signals were amplified, filtered at 300–3,000 Hz, and processed by a data collection system (CED 1401; Cambridge

Instruments). Stored recordings were analyzed offline with Spike2 software (version 7.02; Cambridge Electronic Design). Extracellular single-unit recording methods and identification of wide dynamic range (WDR) neurons have been described previously (16,18). Briefly, WDR neurons were first identified by their general response to a range of low- and high-threshold peripherally evoked stimuli (that is, light brushing with a cotton-tipped swap and pinching with sharp forceps) applied to each neuron's cutaneous receptive field. Following WDR neuron identification, we mapped the cutaneous receptive field surface area of each neuron on an outline of the dorsal surface of the rat hindquarters by lightly brushing, pinching and probing with von Frey filaments (18,22). The areas of each receptive field were measured using NIH ImageJ (free software available at http://rsbweb.nih.gov/ij/). An arbitrary standard unit for area was assigned and used for quantitative comparison between treatment groups. The following stimuli were then applied: phasic brush (PB) stimulation of the skin with a cotton applicator, compressive pressure (144 g/mm^2), and increasing force (0.04, 0.16, 0.4, 0.6, 1.0, 4.0, 6.0, 15.0, 26.0 g). These stimulus modalities are reflective of human nociceptive testing (23,24). We confirmed that responses were maximal by stimulating the primary receptive field of each unit and ensured that isolated units remained stable during recording by using software wave template matching routines. The activities of 4–6 WDR units/animal were recorded from the lumbar enlargement (~500–800-µm deep), which yielded 15–16 units/treatment group.

Statistical Analyses

For analyses, an α value of $p < 0.05$ was used to determine significance. One-way repeated analysis of variance (ANOVA) followed by Bonferroni *post hoc* correction was used for analyses of tactile and heat sensitivity over the studied time course. Mann-Whitney *U* tests were used for treatment group comparisons at specific

experimental time points. For electrophysiological data, two-tailed analyses using parametric or nonparametric tests were used, as appropriate. We used repeated measures ANOVA or Kruskal-Wallis one-way ANOVA on ranks, followed by Bonferroni or Dunn *post hoc* tests. Data management and statistical analyses were performed using SigmaPlot (version 12; Systat) and Microsoft Office Excel 2011. Data in the text are described as mean ± standard deviation (SD). All graphs were plotted as mean ± standard error of the mean (SEM) using SigmaPlot (version 12).

RESULTS

Intrathecal Injection Delivers AAV to DRG Neurons without Infecting Spinal Cord Dorsal Horn Neurons

We have previously designed and successfully utilized the AAV2/5-shRNA-Nav1.3 vector to specifically knock down Nav1.3 expression *in vivo* by administering this AAV vector directly to DRG neurons (that is, through an intraganglionic injection technique) (5). To further extend these studies using a minimally invasive, clinically applicable delivery method, we used an intrathecal injection approach that others have described to allow AAV to effectively transduce DRG neurons without significantly affecting pain thresholds (25,26). To confirm transduction efficiency and neuronal target specificity in our study, we analyzed spinal cord and DRG tissue collected from animals at the experimental endpoint (3 wks post-STZ injection). We quantified the percentage of GFP-positive neuronal profiles in tissue sections of L4-L5 DRGs, which contribute to the innervation of the hindquarters and hindpaw dermatomes. Using NeuN-immunopositive staining as a neuronal colocalization marker, we observed an average transduction rate of 50.3 ± 3.1% of DRG neurons (Figure 2A).To determine whether AAV infection was restricted to peripheral DRG neurons, we also performed a histological study of spinal cord tissues collected from AAV-injected animals.

Three weeks after AAV injection, spinal cord tissue from the lumbar enlargement L4–L6 was processed and examined for NeuN-immunopositive cells that were colabeled with GFP-expressing cells (Figure 2B). We did not detect any NeuN-immunopositive neurons with GFP expression, an indication that intrathecal delivery of AAV2/5 did not lead to infection of neurons in the spinal cord dorsal horn. Admittedly, we cannot exclude the possibility that AAV delivered intrathecally could have infected an undetectable small number of spinal cord neurons (26). Interestingly, we observed GFP-labeled primary afferents in several regions of the spinal cord, distributed in a fibrous pattern throughout the dorsal columns, the dorsal horn, and into the ventral horn (Figure 2B; white arrows). In some tissue sections, GFP-labeled afferents appeared within the dorsal root nerve tissue (image not shown), demonstrating that infected GFP-labeled DRGs project axons into the spinal cord.

Intrathecal Injection of AAV2/5-shRNA-Nav1.3 Reduces Nav1.3 mRNA Expression in Lumbar DRGs

Nav1.3 mRNA and protein expression increase in DRGs from STZ-induced diabetic rats. To determine whether AAV2/5-shRNA-Nav1.3 delivered intrathecally can achieve Nav1.3 knockdown *in vivo*, we collected DRG tissue from a subpopulation of animals from the two experimental diabetic groups 3 wks post-STZ injection (control shRNA-scrambled [-Sc] or shRNA-Nav1.3) (Figure 2C). Total RNA was extracted from L4–L5 DRGs for quantification of Nav1.3 mRNA content (n = 8 ganglions/group). Relative Nav1.3 mRNA expression levels were calculated from total RNA content. Nav1.3 mRNA expression significantly decreased in DRGs collected from animals administered AAV-shRNA-Nav1.3 compared with control shRNA-Sc ($p < 0.05$; 18.7%). It is important to note that this analysis used complementary DNA (cDNA) prepared from whole dorsal root ganglion,
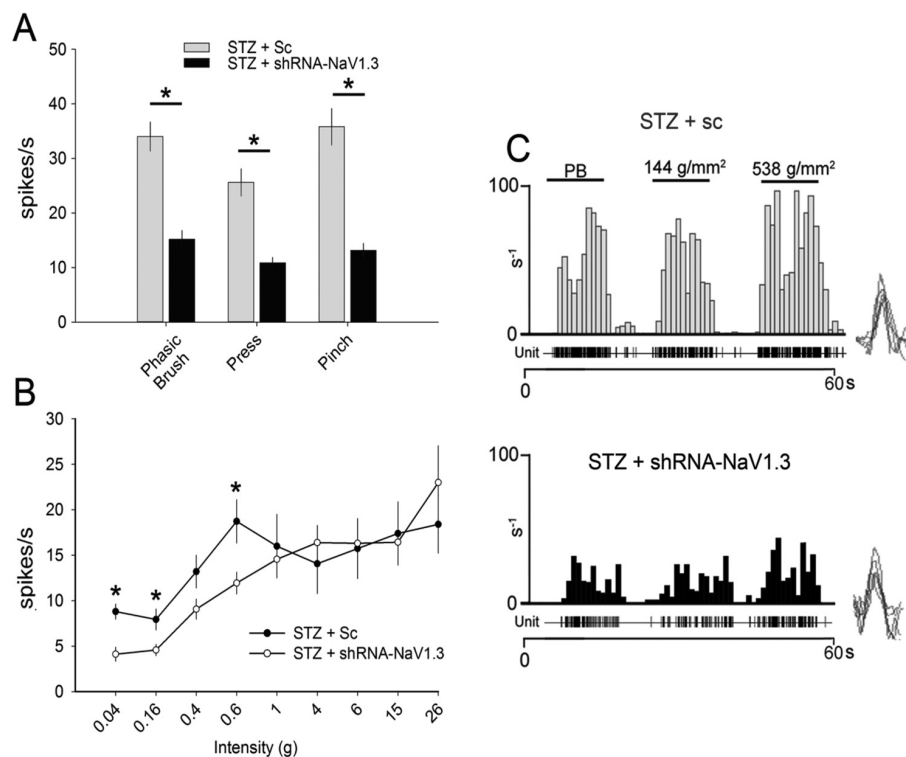
which includes both infected neurons and noninfected cells (for example, noninfected neurons and glia). Thus, the observed reduction in mRNA expression is an underestimation of the actual effect of shRNA incorporation on an individual neuronal level.

Nav1.3 Knockdown Reduces Nociceptive Hyperexcitability Associated with Diabetic Neuropathic Pain

To test the peripherally evoked response of WDR neurons in animals with diabetic neuropathic pain, we sampled units from dorsal horn laminae IV–V (1,27). We identified WDR neurons by their response to both low- and high-threshold peripheral stimuli applied to their cutaneous receptive fields (1,27). In

Figure 3. Peripherally-evoked responses of wide–dynamic range units. (A) Application of phasic brush, press, pinch, and (B) Von Frey filaments applied to cutaneous receptive fields of WDR neurons evoked single-unit firing activity in diabetic animals. Viral-mediated knockdown of NAV1.3 attenuated the responsiveness of diabetic WDR neurons (*$p < 0.05$; n = 16 cells/group). (C) A representative peristimulus histogram shows the peripherally evoked response of WDR single units to phasic brush (PB), compressive press (144 g/mm^2), and pinch (538 g/mm^2). Graphs are mean ± SEM.

diabetic animals, peripheral stimulus consisting of PB, press, and pinch produced mean spike frequencies between 35 and 40 Hz (PB, 33.9 ± 10.7 Hz; press, 25.6 ± 10.0 Hz; pinch, 35.8 ± 13.4 Hz) (Figure 3A). In contrast, injection with AAV-shRNA-Nav1.3 in diabetic animals produced mean spike activities between 10% and 16% (PB, 15.2 ± 6.5 Hz; press, 10.8 ± 3.9 Hz; pinch, 13.1 ± 5.2 Hz), which was a significant reduction in firing frequency across these modalities by 50% compared with control STZ animals ($p < 0.05$; n = 16 cells/group). Similarly, compared with STZ animals receiving control shRNA-Sc, Nav1.3 knockdown with AAV-shRNA-Nav1.3 intrathecal injection resulted in a significant decrease in evoked single-unit activity in response to three Von Frey filament intensities (Fig-
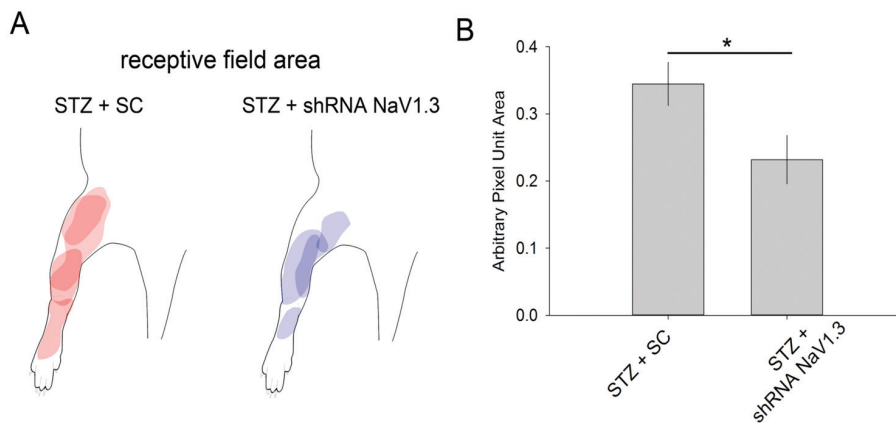
A

receptive field area

STZ + SC   STZ + shRNA NaV1.3

B

Figure 4. Cutaneous receptive fields of WDR units. (A) A representative map shows sampled WDR neuron receptive fields from each group. (B) STZ-induced diabetic animals exhibited enlarged receptive fields, as observed previously (41). Viral-mediated knockdown of Nav1.3 (with shRNA-Nav1.3) reduced the size of the enlarged receptive field compared with receptive fields in animals that received control, scrambled vectors (shRNA-Sc) (*$p < 0.05$; n = 16). Graph is mean ± SEM.

ure 3B), which we applied to hind limb cutaneous fields ($p < 0.05$; 0.04 g, 8.8 ± 3.2 versus 4.1 ± 3.07 Hz; 0.16 g, 7.9 ± 4.5 versus 4.5 ± 2.5 Hz; 0.6 g, 18.7 ± 9.2 versus 11.9 ± 4.8 Hz). A representative peristimulus histogram of WDR responses (spikes per 1-s bin) is shown in Figure 3C for both STZ + Sc and STZ + shRNA-Nav1.3 groups.

Our previous study demonstrated that the receptive fields of dorsal horn units expand in animal models of diabetic neuropathic pain (16). To test whether Nav1.3 knockdown induces changes in receptive fields of WDR neurons (Figure 4), we mapped cutaneous receptive fields of sampled neurons by light brushing, pinching and probing with Von Frey filaments (see Materials and Methods). As shown in representative maps, the receptive field areas in diabetic animals demonstrated enlarged receptive fields (28) (Figure 4A). Injection of AAV-shRNA-Nav1.3 resulted in a qualitative reduction in these receptive field sizes (Figure 4B). Quantification demonstrated that AAV-shRNA-Nav1.3 injection in diabetic animals decreased cutaneous receptive field areas compared with control viral-injected STZ animals (Figure 4B) ($p < 0.05$; 0.23 ± 0.11 versus 0.41 ± 0.22 pixel unit area; n = 16/group).

Nav1.3 Knockdown in DRG Neurons Reduces Neuropathic Tactile Allodynia in Diabetic Rats

Injection of STZ is an established model for type I diabetes mellitus in adult rats (16). We have previously demonstrated that rats injected intraperitoneally with STZ develop high blood glucose (hyperglycemia) as early as 4 d following injection (16,28). Moreover, these hyperglycemic rats exhibit a gradual reduction in tactile pain thresholds within 1 wk following STZ injection, and by the third week exhibit significant neuropathic tactile allodynia that is characteristic of painful diabetic neuropathy (16,17). In this study, all animals developed significant hyperglycemia by the experimental endpoint at 3 wks after STZ injection (blood glucose range, 293–600 mg/dL; mean, 575.6 ± 16 mg/dL; n = 27 [also see Materials and Methods]). All animals gained body mass over the 3 wk experimental time course, despite the development of hyperglycemia (baseline versus 3 wks post-STZ injection: $p < 0.05$; 231.4 ± 12.6 versus 264.6 ± 44.0 g).

To determine whether knockdown of Nav1.3 in rats with diabetes can attenuate tactile allodynia, we injected rats with either shRNA-Nav1.3 4 d after STZ-induction (n = 14) or shRNA-Sc (n = 13).

We measured tactile withdrawal thresholds of the ipsilateral hindpaw (for example, AAV injected side) at three time points: baseline (before any STZ induction), 1 wk and 3 wks post-STZ injection (Figure 5A). Rats injected with control shRNA-Sc exhibited a significant drop in tactile withdrawal thresholds by 1 wk after STZ injection compared with baseline ($p < 0.05$; 10.4 ± 3.0 versus 20.1 ± 5.1 g), which progressively worsened by wk 3 ($p < 0.05$; 4.1 ± 6.6 versus 20.1 ± 5.1 g). STZ-animals injected with shRNA-Nav1.3 demonstrated a comparable drop in tactile withdrawal threshold 1 wk following STZ injection compared with baseline ($p < 0.05$; 9.03 ± 3.3 versus 20.0 ± 5.1 g). However, by 3 wks, animals with shRNA-Nav1.3 injection showed a significant reversal of tactile allodynia, with the withdrawal threshold increasing by nearly three-fold compared with control shRNA-Sc–treated animals ($p < 0.05$; 13.3 ± 5.9 versus 4.1 ± 6.6 g) (Figure 5A). The delayed onset of the effect of AAV-mediated Nav1.3 knockdown is likely due to the 2–3-wk time course required for neuronal expression of the vector, an observation we have reported previously (12).In agreement with our previous study (18), heat threshold testing revealed no significant effect of STZ-induced diabetes over the 3-wk time course of the study (shRNA-Sc, $p > 0.05$; 11.7 ± 2.3 versus 8.1 ± 3.3 versus 10.6 ± 1.3 s; shRNA-Nav1.3, $p > 0.05$; 10.1 ± 2.9 versus 10.4 ± 2.6 versus 9.9 ± 1.7 s; n = 4–5/group) (Figure 5B).Together, these behavioral assessments demonstrate that intrathecal delivery of AAV-shRNA-Nav1.3 results in knockdown of Nav1.3 misexpression in lumbar DRGs that is associated with significantly reduced diabetic neuropathic tactile allodynia.

DISCUSSION

Diabetes mellitus is a global epidemic, affecting more than 50 million individuals (16). Neuropathic pain represents a major complication of chronic diabetes, and current medical treatments have had limited effectiveness in managing diabetic neuropathic pain. Here, we sought

to further address the unmet medical need of diabetic neuropathic pain using gene therapy. We have shown that Nav1.3 is upregulated within DRG neurons of STZ-induced diabetic rats, suggesting its mechanistic role in neuropathic pain (16). As a result of its biophysical properties, Nav1.3 increases the excitability of cells in which it is expressed and has been previously shown to contribute to neuropathic pain (29). We hypothesized that a gene therapy approach to knockdown Nav1.3 expression in DRG neurons would attenuate neuropathic pain in diabetic rats. To this end, we used our validated AAV-shRNA-Nav1.3 vector, which was administered to diabetic rats using a clinically applicable intrathecal injection method (7,12). Three weeks after injection, we observed robust transduction of multiple DRG neurons along the lumbar enlargement without an effect on transduction of spinal cord neurons. Functional testing in postsynaptic neurons in the spinal cord demonstrated a concomitant reduction in the excitability of the dorsal horn neurons to which DRG neurons project, and behavioral testing showed a decrease in neuropathic tactile allodynia. Taken together, our findings support a novel gene therapy strategy that specifically targets misexpressed sodium channels that contribute to diabetic neuropathic pain.

Our results demonstrate that Nav1.3 sodium channels contribute to diabetic neuropathic pain. Previous studies have shown that there is a significant and persistent increase in mRNA and protein expression of Nav1.3 within DRG neurons (25). Expression of the β3 sodium channel subunit, which forms a complex with Nav1.3, also increased in DRG neurons of STZ-induced diabetic rats, an observation consistent with the insertion of Nav1.3 into cellular membranes (5). Importantly, Nav1.3 drives a fast-recovering TTX-sensitive current (for example, the channel rapidly recovers from inactivation) and produces a "ramp response" to small stimuli, properties that support high-frequency repetitive firing in neu-
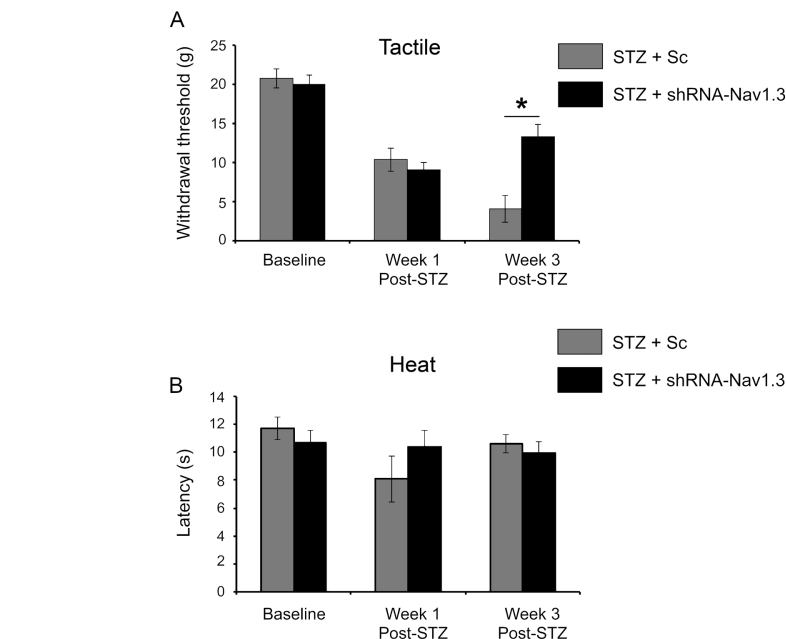

Figure 5. Tactile and heat pain thresholds. A blinded observer performed pain behavioral testing for (A) tactile allodynia and (B) heat hyperalgesia at baseline (prior to STZ induction of diabetes), and 1 and 3 wks after STZ induction. One week after STZ induction there was a significant decrease in the tactile withdrawal threshold for all animals compared with baseline (see results), demonstrating the presence of neuropathic tactile allodynia. By 3 wks after STZ induction, administration of AAV-shRNA-Nav1.3 in diabetic animals resulted in a partial attenuation of diabetic-induced tactile allodynia compared with animals that received control, scrambled vector (shRNA-Sc) (*$p < 0.05$). There was no effect of STZ-induced diabetes or treatment on heat pain thresholds.

rons associated with neuropathic pain. Despite emerging evidence that Nav1.3 may contribute to abnormal nociception, no published study has directly reported on the functional relevance of diabetic-induced Nav1.3 misexpression. We observed reduced neuronal excitability of dorsal horn neurons and reduced behavioral evidence of tactile allodynia in diabetic rats 3 wks following vector administration. These observations suggest that DRG neurons infected with AAV-shRNA-Nav1.3 had lower levels of functional Nav1.3 channels than those that received the control vector. AAV-shRNA-sc. Nav1.3 is one of multiple sodium channel isoforms expressed in DRG neurons that are TTX-S. The TTX-S sodium currents in DRG neurons, normal or diabetic, are a composite of Nav1.1, -1.3, -1.6 and -1.7. Isoform-specific blockers are unavailable for single-

cell–level electrophysiology studies, and because of the dilution effect of other Nav isoforms, patch clamp studies reveal only changes in current density requiring a very large number of cells and do not identify the isoform that is knocked down. Calcium imaging, or voltage-sensitive dyes, have emerged as powerful technologies in neurophysiology, but this approach still fails to achieve the resolution necessary to detect the changes in functional expression of specific Nav isoforms. A study on Nav currents in axotomized DRG neurons (12), while detailed, documented changes in the functional expression of sodium channels but did not discern specific isoform changes, such as Nav1.3. Taken together, physiological methods lack sufficient resolution to definitively identify Nav isoforms from composite TTX-S currents in DRG neu-

rons. Thus, in our previous gene therapy study we chose to verify the functional efficacy of the Nav1.3 knockdown construct in HEK293 cells, in which we definitively attributed changes in current density to the Nav1.3 isoform (13,30). In the present study using the same construct, we showed a decrease in Nav1.3 mRNA expression in DRG tissues following viral transduction of approximately 50% of L4–L5 DRG neurons and concomitant reductions of both dorsal horn neuron hyperexcitability and tactile allodynia. Together, our results suggest that these physiological changes in DRG neurons and in tactile allodynia are attributable, at least in part, to knockdown of Nav1.3. We did not observe a significant change in heat withdrawal sensitivity in STZ-induced diabetic animals. This finding is in agreement with other reports in the literature that have shown that STZ-induced diabetic rats exhibit no or little change in heat pain (5,13,31). However, others have shown that STZ-induced diabetes in rats can lead to the development of heat hyperalgesia (32). The discrepancy between these findings might be explained by the multiple pathological mechanisms that contribute to the development of diabetic neuropathic pain (for example, peripheral nerve damage, secondary vascular disease, hypoxia), such that even small changes in the pathogenesis of diabetes could produce large variations in specific sensory modalities, such as heat detection (16,33,34). For example, in studies that report normal thermal sensitivity, small DRG neurons with thinly myelinated Aδ fibers or unmyelinated C-fiber afferents, which carry thermal nociceptive information, may have been minimally unaffected, whereas in other cases of diabetes, C fibers may have become more substantially affected (35). Alternatively, the instrumentation and assessment used to detect the noxious heat threshold (for example, a radiant heat stimuli was used in this study) might have limited sensitivity in this assay. The Hargreaves method cannot assess subthreshold heat intensities or

responses to prolonged heat exposure (36,37). Taken together, it is clear that further studies are required to firmly establish whether heat hyperalgesia is affected in an STZ model of diabetes. Nav1.3 is preferentially upregulated in larger DRG neurons that are responsible for transmitting tactile sensory information in our model of STZ-induced diabetic neuropathic pain (21,38). In agreement with published reports (12), we observed GFP-labeled afferent fibers within the intermediate zone of the dorsal horn, dorsal columns and attached nerve roots. In some cases, sparsely distributed GFP-labeled fibers were observed in the ventral horn. Together, these findings suggest that some of the AAV-infected DRG neurons were of the medium- and large-diameter range and are cells that are generally considered to carry nonnoxious, discriminatory and proprioceptive information (16). Consistent with this observation, we demonstrate that targeted knockdown of Nav1.3 expression results in reducing tactile allodynia (for example, the presence of pain from typically nonpainful stimuli).It is not surprising that AAV-shRNA injection resulted in only a partial recovery of tactile pain thresholds. Expression of other sodium channel isoforms is upregulated in DRG neurons in the STZ-induced diabetic model of pain, for example, Nav1.7, Nav1.6 and Nav1.9 (26); these other channels may also contribute to altering the intrinsic firing properties of DRGs associated with neuropathic pain. In addition, AAV transduced only a subpopulation of DRG neurons along the lumbar enlargement—the remaining uninfected DRG cells would continue to display hyperexcitability *in vivo* and contribute to ongoing abnormal pain. Emerging evidence also supports a central nervous system (CNS) contribution to diabetic neuropathic pain, with upregulation of Nav1.3 expression in other regions of the CNS (for example, spinal cord dorsal horn and thalamus) following peripheral nerve or spinal cord injury (12,18,26,39). In our study, administration of AAV ap-

peared to affect only DRG neurons, and thus other CNS nociceptive systems would continue to contribute to the pain phenotype.

CONCLUSION

In summary, our results demonstrate that intrathecal administration of AAV-mediated gene therapy is a promising therapeutic strategy. Although previous studies have targeted sodium channels in DRG neurons in models of diabetes, a lack of Nav isoform specificity has limited these studies' translational relevance and limited their mechanistic insights into neuropathic pain. In this regard, our findings are novel, demonstrating a contribution of Nav1.3 misexpression in diabetic neuropathic pain. Moreover, by using a clinically feasible intrathecal delivery method, we have improved upon our previous viral-delivery platform. Compared with intraganglionic injections (40), the reported intrathecal injection method is rapid, less invasive, and increases the bioavailability of the vector to multiple DRG neurons, with no or negligible infection of spinal cord tissue. Importantly, our study demonstrates that intrathecal administration of AAV-mediated gene therapy is effective, which provides broad support for the utility of viral-mediated strategies to address other hyperexcitability disorders associated with chronic neuropathic diseases.

DISCLOSURE

The authors declare they have no competing interests as defined by *Molecular Medicine*, or other interests that might be perceived to influence the results and discussion reported in this paper.

REFERENCES

1. Zilliox L, Russell JW. (2011) Treatment of diabetic sensory polyneuropathy. *Curr. Treat. Options Neurol.* 13:143–59.
2. Dib-Hajj SD, Black JA, Waxman SG. (2009) Voltage-gated sodium channels: therapeutic targets for pain. *Pain Med.* 10:1260–9.
3. Dib-Hajj SD, Cummins TR, Black JA, Waxman SG. (2010) Sodium channels in normal and pathological pain. *Annu. Rev. Neurosci.* 33:325–47.
4. Black JA, *et al.* (1999) Upregulation of a silent sodium channel after peripheral, but not central, nerve injury in DRG neurons. *J. Neurophysiol.* 82:2776–85.
5. Samad OA, *et al.* (2013) Virus-mediated shRNA knockdown of Na(v)1.3 in rat dorsal root ganglion attenuates nerve injury-induced neuropathic pain. *Mol. Ther.* 21:49–56.
6. Waxman SG, Kocsis JD, Black JA. (1994) Type III sodium channel mRNA is expressed in embryonic but not adult spinal sensory neurons, and is reexpressed following axotomy. *J. Neurophysiol.* 72:466–70.
7. Cummins TR, *et al.* (2001) Nav1.3 sodium channels: rapid repriming and slow closed-state inactivation display quantitative differences after expression in a mammalian cell line and in spinal sensory neurons. *J. Neurosci.* 21:5952–61.
8. Waxman SG, Hains BC. (2006) Fire and phantoms after spinal cord injury: Na+ channels and central pain. *Trends Neurosci.* 29:207–15.
9. Lindia JA, Kohler MG, Martin WJ, Abbadie C. (2005) Relationship between sodium channel NaV1.3 expression and neuropathic pain behavior in rats. *Pain.* 117:145–53.
10. Nassar MA, *et al.* (2006) Nerve injury induces robust allodynia and ectopic discharges in Nav1.3 null mutant mice. *Mol. Pain.* 2:33.
11. Yin R, *et al.* (2015) Voltage-gated sodium channel function and expression in injured and uninjured rat dorsal root ganglia neurons. *Int. J. Neurosci.* 2015, Apr 7 [Epub ahead of print].
12. Craner MJ, Klein JP, Renganathan M, Black JA, Waxman SG. (2002) Changes of sodium channel expression in experimental painful diabetic neuropathy. *Ann. Neurol.* 52:786–92.
13. Shah BS, *et al.* (2001) Beta3, a novel auxiliary subunit for the voltage gated sodium channel is upregulated in sensory neurones following streptozocin induced diabetic neuropathy in rat. *Neurosci. Lett.* 309:1–4.
14. Szolcsanyi J, Pinter E. (2013) Transient receptor potential vanilloid 1 as a therapeutic target in analgesia. *Expert Opin. Ther. Targets.* 17:641–57.
15. Glorioso JC, Fink DJ. (2009) Gene therapy for pain: introduction to the special issue. *Gene Ther.* 16:453–4.
16. Tan AM, *et al.* (2012) Maladaptive dendritic spine remodeling contributes to diabetic neuropathic pain. *J. Neurosci.* 32:6795–807.
17. Morrow TJ. (2004) Animal models of painful diabetic neuropathy: the STZ rat model. *Curr. Protoc. Neurosci.* Chapter 9:Unit 9.18.
18. Fischer TZ, Tan AM, Waxman SG. (2009) Thalamic neuron hyperexcitability and enlarged receptive fields in the STZ model of diabetic pain. *Brain Res.* 1268:154–61.
19. Persson AK, Gasser A, Black JA, Waxman SG. (2011) Na1.7 accumulates and co-localizes with phosphorylated ERK1/2 within transected axons in early experimental neuromas. *Exp. Neurol.* 230:273–9.
20. Chaplan SR, Bach FW, Pogrel JW, Chung JM, Yaksh TL. (1994) Quantitative assessment of tactile allodynia in the rat paw. *J. Neurosci. Methods.* 53:55–63.
21. Hargreaves K, Dubner R, Brown F, Flores C, Joris J. (1988) A new and sensitive method for measuring thermal nociception in cutaneous hyperalgesia. *Pain.* 32:77–88.
22. Chang YW, Tan A, Saab C, Waxman S. (2010) Unilateral focal burn injury is followed by long-lasting bilateral allodynia and neuronal hyperexcitability in spinal cord dorsal horn. *J. Pain.* 11:119–30.
23. Baumgartner U, Magerl W, Klein T, Hopf HC, Treede RD. (2002) Neurogenic hyperalgesia versus painful hypoalgesia: two distinct mechanisms of neuropathic pain. *Pain.* 96:141–51.
24. Pitcher GM, Henry JL. (2004) Nociceptive response to innocuous mechanical stimulation is mediated via myelinated afferents and NK-1 receptor activation in a rat model of neuropathic pain. *Exp. Neurol.* 186:173–97.
25. Parikh P, *et al.* (2011) Regeneration of axons in injured spinal cord by activation of bone morphogenetic protein/Smad1 signaling pathway in adult neurons. *Proc. Natl. Acad. Sci U. S. A.* 108:E99–107.
26. Xu Q, *et al.* (2012) In vivo gene knockdown in rat dorsal root ganglia mediated by self-complementary adeno-associated virus serotype 5 following intrathecal delivery. *PloS One* 7:e32581.
27. Tan AM, Chang YW, Zhao P, Hains BC, Waxman SG. (2011) Rac1-regulated dendritic spine remodeling contributes to neuropathic pain after peripheral nerve injury. *Exp. Neurol.* 232:222–33.
28. Gjerstad J, Tjolsen A, Hole K. (2001) Induction of long-term potentiation of single wide dynamic range neurones in the dorsal horn is inhibited by descending pathways. *Pain.* 91:263–8.
29. Setacci C, de Donato G, Setacci F, Chisci E. (2009) Diabetic patients: epidemiology and global impact. *J. Cardiovasc. Surg.* 50:263–73.
30. Cummins TR, Waxman SG. (1997) Downregulation of tetrodotoxin-resistant sodium currents and upregulation of a rapidly repriming tetrodotoxin-sensitive sodium current in small spinal sensory neurons after nerve injury. *J. Neurosci.* 17:3503–14.
31. Pertovaara A, Wei H, Kalmari J, Ruotsalainen M. (2001) Pain behavior and response properties of spinal dorsal horn neurons following experimental diabetic neuropathy in the rat: modulation by nitecapone, a COMT inhibitor with antioxidant properties. *Exp. Neurol.* 167:425–34.
32. Raz I, Hasdai D, Seltzer Z, Melmed RN. (1988) Effect of hyperglycemia on pain perception and on efficacy of morphine analgesia in rats. *Diabetes.* 37:1253–9.
33. Courteix C, Eschalier A, Lavarenne J. (1993) Streptozocin-induced diabetic rats: behavioural evidence for a model of chronic pain. *Pain.* 53:81–8.
34. Benbow SJ, Chan AW, Bowsher D, MacFarlane IA, Williams G. (1994) A prospective study of painful symptoms, small-fibre function and peripheral vascular disease in chronic painful diabetic neuropathy. *Diabet. Med.* 11:17–21.
35. Boucek P. (2006) Advanced diabetic neuropathy: a point of no return? *Rev. Diabet. Stud.* 3:143–50.
36. Jain R. (2008) Pain and the brain: diabetic neuropathic pain. *J. Clin. Psychiatry.* 69:e22.
37. Ahlgren SC, Levine JD. (1994) Protein kinase C inhibitors decrease hyperalgesia and C-fiber hyperexcitability in the streptozotocin-diabetic rat. *J. Neurophysiol.* 72:684–92.
38. Chen SR, Pan HL. (2002) Hypersensitivity of spinothalamic tract neurons associated with diabetic neuropathic pain in rats. *J. Neurophysiol.* 87:2726–33.
39. Fischer TZ, Waxman SG. (2010) Neuropathic pain in diabetes—evidence for a central mechanism. *Nat. Rev. Neurol.* 6:462–6.
40. Hains BC, Saab CY, Waxman SG. (2005) Changes in electrophysiological properties and sodium channel Nav1.3 expression in thalamic neurons after spinal cord injury. *Brain.* 128:2359–71.
41. Zhao P, Waxman SG, Hains BC. (2006) Sodium channel expression in the ventral posterolateral nucleus of the thalamus after peripheral nerve injury. *Mol. Pain.* 2:27.